

# A Molecular Dynamics Study of Aqueous Solutions

## II. Cesium Chloride in H<sub>2</sub>O

P. C. Vogel and K. Heinzinger

Max-Planck-Institut für Chemie (Otto-Hahn-Institut), Mainz, Germany

(Z. Naturforsch. **30 a**, 789–796 [1975] ; received April 15, 1975)

Results of a molecular dynamics study of an aqueous CsCl solution are reported. The system consisted of 216 particles, 200 water molecules, 8 cesium ions and 8 chloride ions and was run over 8000 time steps equivalent of  $9 \cdot 10^{-13}$  sec. On the basis of radial pair correlation functions, average potential energy of the water molecules and pair interaction energy distribution the static properties of the first hydration shells of the ions are discussed in detail. The self diffusion coefficient for the water molecules is calculated and compared with NMR measurement as well as with molecular dynamics calculations for pure water at elevated temperatures and pressures.

### I. Introduction

In an earlier paper from this laboratory<sup>1</sup> results of a molecular dynamics study of an aqueous LiCl solution were reported. The calculations were based on a computer program developed by Rahman and Stillinger for pure water<sup>2–4</sup>. The results of these first molecular dynamics calculations of the properties of aqueous solutions seemed promising, and therefore a continuation and expansion of the calculations with some modifications were undertaken.

Essentially, the following modifications were made:

1) The switching function has been removed from the ion-water pair potential, as the strong change in slope between 4 and 5 Å caused by it resulted in some artificial bumps of the calculated properties in this region.

2) The ion-ion interactions are relatively strong compared with all other interactions. Therefore, the ions in the 26 nearest neighbor image boxes were included into the calculations. The switching function for turning off the ion-ion pair potential, which became effective between 4 and 5 Å previously, now starts reducing the interaction potential at about 9.4 Å.

3) The length of the time step was reduced by a factor of three in order to improve the integration of the equations of motion.

4) The radial pair correlation functions between the ions and hydrogen atoms are calculated, giving additional information on the arrangement of water molecules around the ions.

5) The radial pair correlation function between ions of opposite sign is introduced in spite of the rather poor statistical sampling.

6) The average potential of the water molecules in the field of the ions is calculated as a function of the distance.

In this work a CsCl solution was investigated, instead of a LiCl solution, in order to reduce problems in the integration procedure connected with the small mass of Li<sup>+</sup>.

### II. Effective Pair Potentials

The total potential was developed as the sum of effective pair potentials, as in the previous work<sup>1</sup>. The ST2 point charge model was again used for the water molecule<sup>1,3</sup>. Four point charges,  $q = 0.23 e$ , are tetrahedrally arranged around the oxygen atom, which resides in the center of a Lennard-Jones sphere. The two positive charges are at a distance of 1 Å from the oxygen atom and coincide with the masses of the hydrogen atoms, while the two negative charges are located at a distance of 0.8 Å, the central angles remaining those of a tetrahedron ( $109^\circ 28'$ ). The ions are treated as point charges residing at the center of Lennard-Jones spheres. Each of the six pair potentials consists of a Lennard-Jones and a Coulomb term:

$$V_{ij}(r, d_{11}, d_{12}, \dots) = V_{ij}^{LJ}(r) + V_{ij}^C(r, d_{11}, d_{12}, \dots) \quad (1)$$

where  $i$  and  $j$  refer to Cs<sup>+</sup>, Cl<sup>−</sup>, or water.  $r$  denotes the distance between the Lennard-Jones centers of the two particles, and  $d_{\alpha\beta}$  the distances between the point charges of the two water molecules  $i$  and  $j$ , or an ion  $i$  and a water molecule  $j$ .

Reprint requests to Dr. K. Heinzinger, Max-Planck-Institut für Chemie, D-6500 Mainz, Saarstr. 23, P.O.B. 3060.

Table 1. Lennard-Jones parameters used in the calculations. The values are derived by application of Kong's<sup>5</sup> combination rules to data obtained by Hogervorst<sup>6</sup>. The  $\sigma_{ij}$  are given in Å, the  $\epsilon_{ij}$  in units of  $10^{-16}$  erg.

	H <sub>2</sub> O—H <sub>2</sub> O	Cs <sup>+</sup> —Cs <sup>+</sup>	Cl <sup>−</sup> —Cl <sup>−</sup>	Cs <sup>+</sup> —H <sub>2</sub> O	Cl <sup>−</sup> —H <sub>2</sub> O	Cs <sup>+</sup> —Cl <sup>−</sup>
$\epsilon_{ij}$	52.605	185.435	97.7878	84.2381	70.0009	128.935
$\sigma_{ij}$	3.10	3.92	3.36	3.58	3.24	3.65

The Lennard-Jones term of the potential is given in the usual form:

$$V_{ij}^{IJ}(r) = 4 \epsilon_{ij} [(\sigma_{ij}/r)^{12} - (\sigma_{ij}/r)^6]. \quad (2)$$

The values for  $\epsilon_{ij}$  and  $\sigma_{ij}$  used in the calculations are given in Table 1.

The three Coulomb terms for water-water, ion-ion, and ion-water interaction are given by:

$$V_{ww}^C(r, d_{11}, d_{12}, \dots) = S_w(r) q^2 \sum_{\alpha, \beta=1}^4 (-1)^{\alpha+\beta} / d_{\alpha, \beta}, \quad (3)$$

$$V_{++}^C(r) = \left( \begin{smallmatrix} + \\ + \end{smallmatrix} \right) e^2 (100 S_I + 1)^{-1} r^{-1}, \quad (4)$$

$$V_{+-}^C(r, d_{+1}, d_{+2}, \dots) = \left( \begin{smallmatrix} + \\ - \end{smallmatrix} \right) \sum_{\alpha=1}^4 (-1)^\alpha q e / d_{+\alpha}. \quad (5)$$

The choice of  $\alpha$  and  $\beta$  odd for positive and even for negative charges yields the correct sign. The switching function,  $S_w(r)$  in  $V_{ww}^C$  is introduced to prevent an unlimited increase in the pair potential, should two of the point charges overlap<sup>2</sup>. The switching function  $S_I$  in the ion-ion pair potential is introduced to attenuate the interaction strongly near the cutoff distance. Both switching functions have the same form:

$$\begin{aligned} S_i &= 0 & (\text{where } r < R_i^L), \\ &= (r - R_i^L)^2 (3 R_i^U - R_i^L - 2r) / (R_i^U - R_i^L)^3 & (\text{where } R_i^L \leq r \leq R_i^U), \\ &= 1 & (\text{where } R_i^U < r) \end{aligned} \quad (6)$$

where  $i$  denotes either  $w$  or  $I$ . The corresponding four constants,  $R_i$ , have been chosen to be:

$$\begin{aligned} R_w^L &= 2.1061 \text{ Å}, & R_w^U &= 3.1287 \text{ Å}, \\ R_I^L &= 9.3678 \text{ Å}, & R_I^U &= 28.1034 \text{ Å}. \end{aligned}$$

Some pair potentials are shown in Figure 1. For actual calculations, the pair potential of the water-water interactions was taken to be zero beyond a cutoff distance of 7.11 Å. The cutoff distance of the ion-water interactions was chosen to be half the side length of the basic periodic box, 9.4 Å.

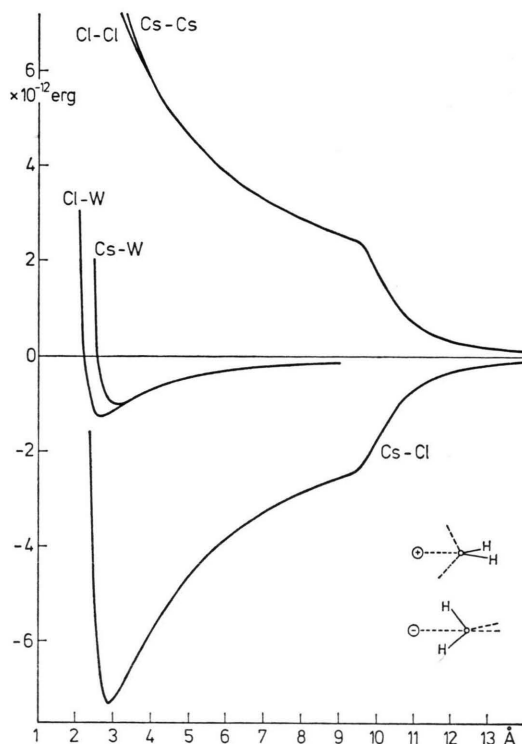


Fig. 1. Effective pair potentials for ion-ion and ion-water interactions according to Eqs. (2), (4) and (5) with  $\sigma$  and  $\epsilon$  values as given in Table 1. The ion-water pair potentials are drawn for water molecule orientations as shown in the lower part of the figure.

Because of the long range nature of the ion-ion interaction it was decided to include the ions in the nearest neighbor image boxes into the ion-ion pair potential in order to stabilize the system. The attenuation of the ion-ion pair potential by a switching function was maintained. Compared with the previous work<sup>1</sup>, it is being turned on at a greater distance, 9.4 Å, and reduces the pair potential by a factor of 100 at 28.1 Å.

### III. Details of the Calculations

The molecular dynamics calculations were performed using a modification of the computer program of Rahman and Stillinger<sup>2</sup> as in the earlier

work<sup>1</sup>. The 216 particle system consisted of 200 water molecules, 8 Cs<sup>+</sup> and 8 Cl<sup>-</sup> ions, which yields a ca. 2.2 M solution with a density of 1.25 g/cm<sup>3</sup> and a resulting periodic box of side length 18.74 Å.

The unit parameters used to integrate the equations of motion were:

mass  $2.99 \times 10^{-23}$  g;  
length  $2.82 \times 10^{-8}$  cm;  
energy  $2.00 \times 10^{-14}$  erg;  
time step  $1.00 \times 10^{-4} \sigma(m/\epsilon)^{1/2} = 1.09 \times 10^{-16}$  sec.

The translational and rotational temperature of the water molecules and of both kinds of ions were kept in the range of 295–305 K by checking after each time step and when necessary adjusting the velocities of the particles involved. The system was run altogether 13000 time steps, with the collection of data beginning after 5000 time steps of equilibration.

## IV. Results and Discussion

### A) Radial Pair Correlation Functions

The radial pair correlation functions,  $g_{\text{CsO}}(r)$ ,  $g_{\text{CsH}}(r)$ ,  $g_{\text{ClO}}(r)$ ,  $g_{\text{ClH}}(r)$ , and  $g_{\text{OO}}(r)$ , giving the relative oxygen and hydrogen atom densities about Cs<sup>+</sup>, Cl<sup>-</sup>, and water molecule oxygen respectively, obtained from our molecular dynamics calculations, are shown in Figures 2–4. Also plotted are the running integrations of the total number of water molecules, oxygen and hydrogen atoms in a sphere of radius  $r$  about the central atom X, given by

$$n_{\text{XY}}(r) = 4\pi\varrho_0 \int_0^r r'^2 g_{\text{XY}}(r') dr' \quad (7)$$

where Y is either O or H, and  $\varrho_0$  is the average number density of water molecules.

The interionic radial pair correlation function  $g_{\text{CsCl}}(r)$  and the corresponding running integration number  $n_{\text{CsCl}}(r)$  are given in Figure 5. Due to the small number of ions, the statistics are not good. The smooth curve for  $g_{\text{CsCl}}(r)$  drawn in the figure is the result of an averaging process. The original oscillations are indicated by the circles. It is seen that during the 8000 time steps the two ions do not approach closer than 4 Å, the most probable distance being about 8 Å. This indicates that there is no ion pairing and that the number of water molecules between the two counterions is on the average between

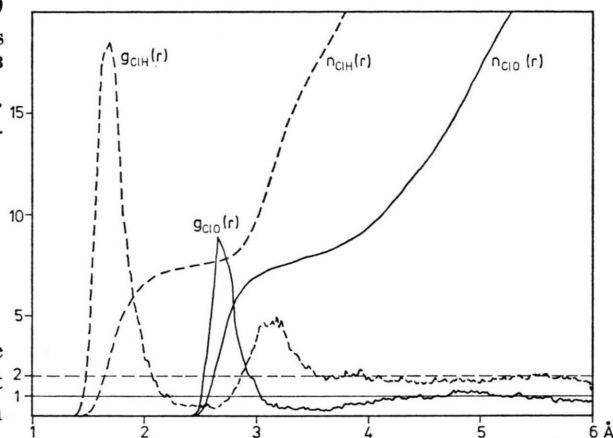


Fig. 3. Radial pair correlation function and running integration number for chlorine-oxygen and chlorine-hydrogen.

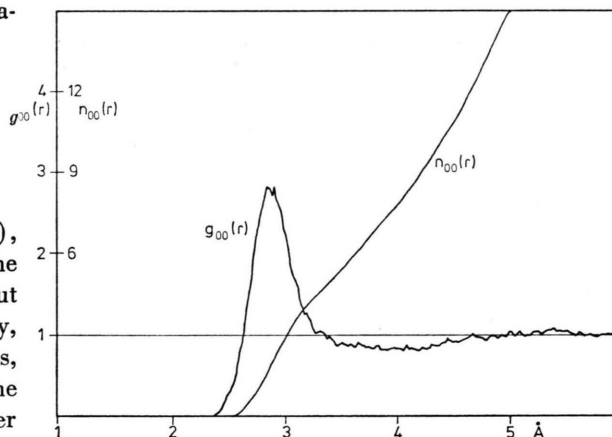


Fig. 4. Radial pair correlation function and running integration number for oxygen-oxygen.

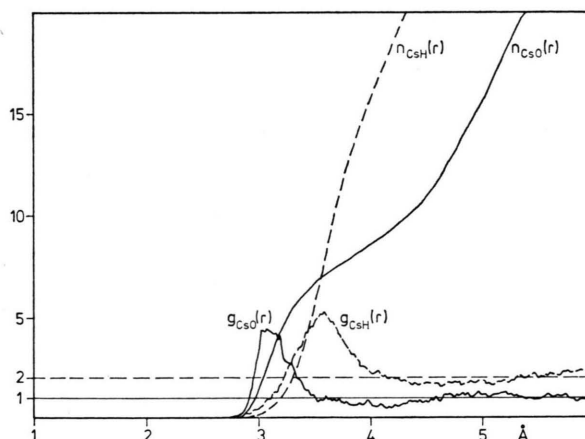


Fig. 2. Radial pair correlation function and running integration number for cesium-oxygen and cesium-hydrogen.

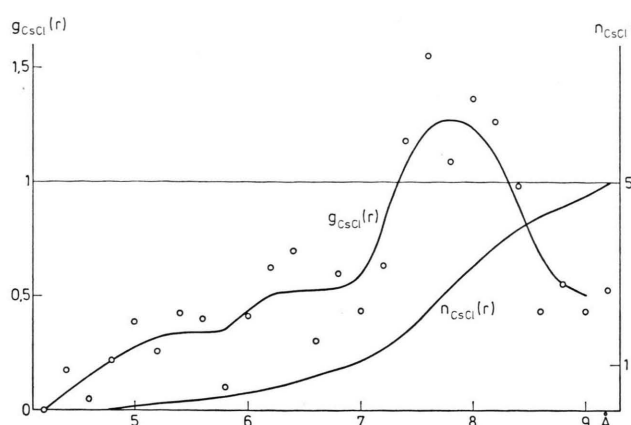


Fig. 5. Radial pair correlation function and running integration number for cesium-chlorine.

two and three as would be expected from the concentration of the solution. The average number of counter ions out to a distance of half the side length of the periodic box is five, a reasonable number considering that the sphere with a radius of this length encompasses roughly half the volume of the periodic box.

The radial pair correlation functions  $g_{\text{CsH}}(r)$  and  $g_{\text{ClH}}(r)$  have been introduced mainly to give additional information about the orientation of the water molecules around the ions and will therefore be discussed in the following section.

The broad peak in  $g_{\text{CsO}}(r)$  with a maximum height of only 4.5 followed by a shallow minimum indicates that the first hydration shell around the  $\text{Cs}^+$  is not very pronounced as one might expect from the generally accepted view that  $\text{Cs}^+$  is negatively hydrated. While the small distance side of the peak is quite sharp, a consequence of the  $r^{-12}$  term in the Lennard-Jones portion of the pair potential, the long distance side decreases relatively slowly. Therefore, there is no real plateau in  $n_{\text{CsO}}(r)$ , and the determination of a hydration number becomes

problematic. Any distance between 3.5 and 4.5 Å might be chosen as the end of the first hydration shell, leading to a hydration number somewhere between 7 and 12. This uncertainty is reflected in the variety of values derived from various experimental methods (see e. g. Bockris and Saluja<sup>7</sup>).

Comparison between these results and the X-ray diffraction studies conducted by Bertagnolli, Weidner and Zimmermann<sup>8</sup> on very concentrated solutions of  $\text{CsF}$  is of very limited value, since at their high concentrations the  $\text{F}^-$  ions, different from  $\text{Cl}^-$ , assume positions in the first hydration shell of the  $\text{Cs}^+$  ions. The value of the  $\text{Cs}^+$ -water distance for their lowest concentration (about 7 moles/l  $\text{H}_2\text{O}$ ) of 3.14 Å falls in the range of the flat top in the  $g_{\text{CsO}}(r)$  peak.

The hydration shell of  $\text{Cl}^-$  is much more pronounced than that of  $\text{Cs}^+$ . The plateaus in  $n_{\text{ClO}}(r)$  and  $n_{\text{ClH}}(r)$  lead to a hydration number of  $8 \pm 1$  for  $\text{Cl}^-$ . In the previous work on  $\text{LiCl}$ <sup>1</sup>, a  $\text{Cl}^-$  hydration number of  $6 \pm 1$  was found in spite of the poor statistics, in agreement with the X-ray and neutron diffraction investigations of Narten, Vaslow, and Levy<sup>9</sup>. Since it is hard to believe that this agreement was fortuitous, the change in the hydration number about the  $\text{Cl}^-$  is expected to result from the change of the positive ion from  $\text{Li}^+$  to  $\text{Cs}^+$ . Further calculations of the alkali halide solutions should provide a more definitive information on the effect of cation size on hydration shell structure of anions, and vice versa, at the concentrations studied here.

The radial pair correlation function for the water molecules,  $g_{\text{OO}}(r)$ , in the  $\text{CsCl}$  solution shows features of pure water at high temperatures, as well as of water under high compression as obtained with molecular dynamics calculations by Rahman and Stillinger for ST2 water under these conditions<sup>3,4</sup>. Position and height of maxima  $\{r(M), g_{\text{OO}}(M)\}$  and minima  $\{r(m), g_{\text{OO}}(m)\}$ , the distances where

Table 2. Comparison of characteristic values of  $g_{\text{OO}}(r)$ , numbers of nearest neighbors and diffusion coefficients for three different molecular dynamics calculations, pure water at 118 °C and normal pressure<sup>3</sup>, pure water at 97 °C under high compression<sup>4</sup> and a 2.2 molal  $\text{CsCl}$  solution. In all three cases the ST2 water model has been used.  $R_1$ ,  $r(M)$  and  $r(m)$  give the distances where  $g_{\text{OO}}(r) = 1$ , has maxima or a minimum respectively. The according  $g$ -values are indicated by  $g_{\text{OO}}(M)$  and  $g_{\text{OO}}(m)$ .

Temp. °C	density g/cm <sup>3</sup>	$R_1$ Å	$R_2$ Å	$r(M_1)$ Å	$g_{\text{OO}}(M_1)$	$r(M_2)$ Å	$g_{\text{OO}}(M_2)$	$r(m_1)$ Å	$g_{\text{OO}}(m_1)$	$n$	$D \cdot 10^5$ cm <sup>2</sup> /sec
118	1	2.63	3.34	2.86	2.64	5.29	1.03	3.74	0.84	5.5	8.4
25	2.2 m $\text{CsCl}$	2.66	3.40	2.88	2.81	5.40	1.09	3.94	0.82	8	7.2
97	1.346	2.55	3.35	2.83	2.80	5.40	1.20	4.0	0.70	11.7	6.5

$g_{00}(r) = 1\{R_i\}$ , as well as the number of nearest neighbors  $\{n\}$  and the diffusion coefficients are given in Table 2. The values for water under high compression are not given explicitly in Ref. 4, but are derived from the figures, and therefore may be slightly in error. The hydrogen bond breaking effect is even more pronounced in the CsCl solution than in the 118 °C water calculation, as indicated by the location of the first minimum and second maximum in  $g_{00}(r)$ , which show values similar to the high compression water. On the other hand, the strong pressure effect leading to a remarkably lower value for  $R_1$  and a pronounced minimum,  $g_{00}(m)$ , and a second maximum,  $g_{00}(M_2)$ , are missing. The height of the first maximum,  $g_{00}(M_1)$ , is again higher than in the case of 118 °C water. The intermediate character of the water in the CsCl solution is also seen in the value of the number of nearest neighbors, 8 if counted as usual out to the distance of the first minimum and from the diffusion coefficient. That the ions exert a certain amount of pressure on the water molecules can also be seen from the  $p(V)$  curve, Fig. 12, which shows a pronounced shoulder at about  $+2.8 \times 10^{-13}$  erg (ca. +4 kcal/mole). This shoulder is also found for water under high compression at approximately the same position, although it is lacking in the case of pure water at elevated temperatures and normal pressure.

### B) Orientation of the Water Molecules

The orientation of the water molecules around the ions can be seen from the average value of  $\cos \Theta$  as a function of distance between oxygen atom and ion shown in Figs. 6 and 7, and from the radial pair correlation functions  $g_{\text{CsH}}(r)$  and  $g_{\text{ClH}}(r)$  included in Figs. 2 and 3. For simplicity the definition of  $\Theta$  as given in the legends of Figs. 6 and 7

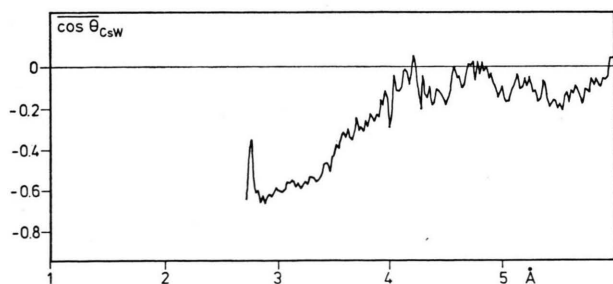


Fig. 6. Average value of  $\cos \Theta$  as a function of distance between oxygen and  $\text{Cs}^+$ .  $\Theta$  is the angle between the two vectors connecting the oxygen atom with  $\text{Cs}^+$  and with the center of mass of the water molecule.

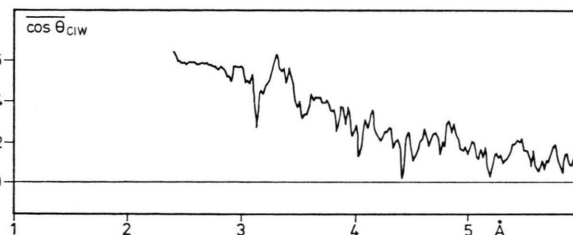


Fig. 7. Average value of  $\cos \Theta$  as a function of distance between oxygen and  $\text{Cl}^-$ .  $\Theta$  is the angle between the two vectors connecting the oxygen atom with  $\text{Cl}^-$  and with the center of mass of the water molecule.

has been changed from that used in the earlier work<sup>1</sup>.

The decrease in the orienting effect of the ions on water molecules in the first hydration shell with increasing ion size is clearly visible in the value of  $\cos \Theta$  for the ion-water interaction, when Cs and Cl are compared. In the case of  $\text{Cs}^+$ -water  $\cos \Theta$  varies from  $-0.62$  to  $-0.46$  over the range of the first peak in  $g_{\text{CsO}}(r)$ . The  $\cos \Theta_{\text{CsW}}$  for the distances between 3.0 and 3.2 Å, the flat top of the  $g_{\text{CsO}}(r)$  peak, is about  $-0.6$ , meaning that a lone pair orbital of the water molecule is directed towards  $\text{Cs}^+$ . The position of the peak in  $g_{\text{CsH}}(r)$  is in good agreement with this conclusion, and the fact that there is only one peak in the  $g_{\text{CsH}}(r)$  excludes any other orientation of the water molecules compatible with  $\cos \Theta_{\text{CsW}} = -0.6$ . The variation of the  $\cos \Theta_{\text{CsW}}$  values between 2.8 and 3.5 Å, together with a certain amount of rotational freedom around the dipole moment of the water molecule, is responsible for the width of the  $g_{\text{CsH}}(r)$  peak. The exceptionally small value of  $\cos \Theta_{\text{CsW}}$  at 2.76 Å occurs at a distance where  $g_{\text{CsO}}(r)$  is nearly identically zero, indicating that it is an isolated occurrence. This energetically unfavorable orientation [see also  $\bar{V}_{\text{CsO}}(r)$  in Fig. 8] may well be caused by the approach of a  $\text{Cs}^+$  and a  $\text{Cl}^-$  with a single water molecule between them, the counter ions having a distance of about 5 Å. The stronger orientational influence of  $\text{Cl}^-$  prevents a similar peak from appearing in  $\cos \Theta_{\text{ClW}}$ .

The relatively strong orienting effect of  $\text{Cl}^-$  compared with  $\text{Cs}^+$  is clearly visible in the  $\cos \Theta_{\text{ClW}}$  in Figure 7. It varies only from 0.6 to 0.55 over the whole range of the peak in  $g_{\text{ClO}}(r)$ , 0.57 corresponding to half the tetrahedral angle showing that a hydrogen atom of the water points directly at the ion. This is strongly confirmed by the peaks in



$g_{\text{ClH}}(r)$ , leading to the same picture of the average ion-water arrangement.

### C) Average Potential Energy

In Figs. 8 and 9 the average potential energies of a water molecule about an ion are shown as a function of the ion-water distance. In addition, the effective pair potentials between the ion and a water

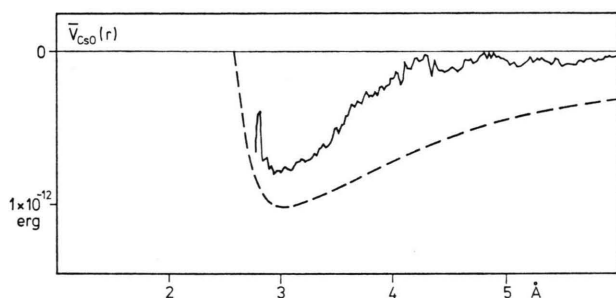


Fig. 8. The average potential energy of a water molecule as a function of the distance between  $\text{Cs}^+$  and the water oxygen. The dashed line shows the effective pair potential for  $\cos \theta_{\text{CsW}} = -1$ .

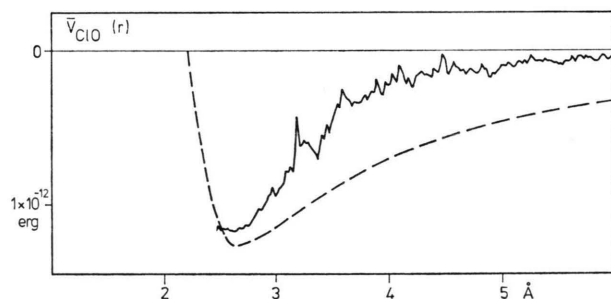


Fig. 9. The average potential energy of a water molecule as a function of the distance between  $\text{Cl}^-$  and the water oxygen. The dashed line shows the effective pair potential for  $\cos \theta_{\text{ClW}} = 1$ .

molecule are given as dashed lines for the case in which  $\cos \theta_{\text{CsW}} = -1$  and  $\cos \theta_{\text{ClW}} = 1$ , the configurations which represent the lowest minimum in the effective pair potential. The comparison between the two curves on each figure shows the strong orienting influence of neighboring water molecules and ions even when the distance between the water molecule and the nearest ion is small. These forces cause the ion-water orientation to become less favorable with increasing ion-water distance, an effect which is also obvious in the  $\overline{\cos \theta}$  curves. The consequence of this is that for small ion-water distances a lone pair orbital or a hydrogen atom is pointed

towards the ion, rather than the dipole moment and the ion being colinear, even though the latter arrangement has a lower energy.

A possible explanation for the peak in  $\bar{V}_{\text{CsO}}(r)$  at 2.76 Å is given above. The result that the  $\bar{V}_{\text{ClO}}(r)$  has a lower energy than the pair potential for the colinear ion-dipole moment arrangement at 2.5 Å arises from the fact that the pair potential for the oxygen-hydrogen- $\text{Cl}^-$  colinear arrangement lies at lower energy at these small distances. The unusually strong "noise" between 4 and 4.5 Å in  $\bar{V}_{\text{CsO}}(r)$  and between 3 and 3.5 Å in  $\bar{V}_{\text{ClO}}(r)$  occurs in areas where  $g_{\text{CsO}}(r)$  and  $g_{\text{ClO}}(r)$  pass through a minimum. Thus, the noise could be due to poor statistical values because of the small number of particles or to the competing influence of both ions on a water molecule located at this distance. The latter view is supported by the fact that the peak in  $g_{\text{CsCl}}(r)$  occurs at the sum of both ion-water distances.

### D) Pair Interaction Energy Distribution

Denoting the average number of pair interactions having an interaction energy in the range  $dV$  by  $p(V) dV$ , the pair interaction energy distribution functions  $p(V)$  for  $\text{Cs}^+$ -water,  $\text{Cl}^-$ -water, and water-water are shown in Figs. 10 to 12.  $p(V)$  is given in arbitrary units. It increases rapidly as  $V$  goes to zero because of the greater number of interactions at large distances where coulombic terms of the potential are small.

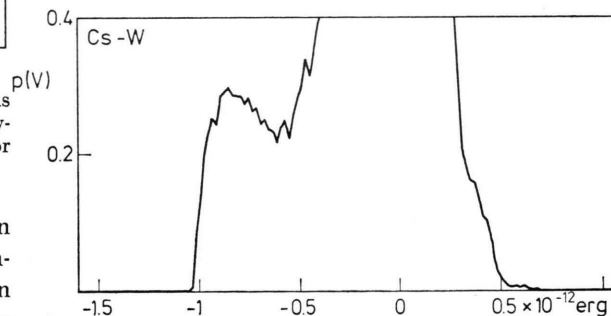


Fig. 10. Pair interaction energy distribution function for cesium-water.  $p(V)$  is given in arbitrary units.

The more or less pronounced hydration shell for  $\text{Cl}^-$  and  $\text{Cs}^+$  respectively are also reflected in the corresponding  $p(V)$  plots. In addition, both curves show a peak which seems beyond statistical noise, at about  $-6 \cdot 10^{-13}$  erg (9 kcal/mole). It is not clear what causes this peak. The positive tail ends at about  $7 \cdot 10^{-13}$  erg in both cases. The positive values

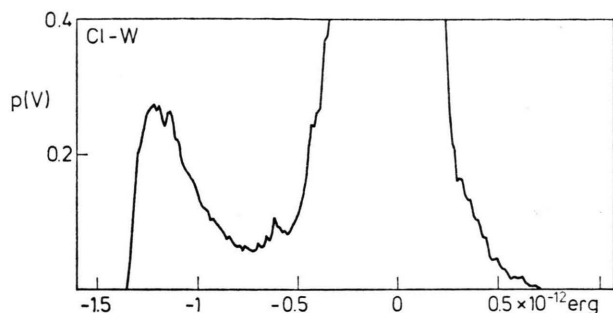


Fig. 11. Pair interaction energy distribution function for chlorine-water.  $p(V)$  is given in arbitrary units.

of the pair potential arise from unfavorable ion-water orientations due to hydration shells of counter ions and from water molecules located in positions intermediate between hydration shells.

The  $p(V)$  plot for water-water interactions shows a plateau at negative energies very similar to the one found by Rahman and Stillinger for pure water at 118 °C and a density of 1 g/cm<sup>3</sup> (see <sup>3</sup>), as well as for pure water at 97 °C and a density of 1.346 g/cm<sup>3</sup> (see <sup>4</sup>). The shoulder at positive energies of about  $2.8 \cdot 10^{-13}$  erg (4 kcal/mole) does not exist for water at normal density but can be seen for the water under high pressure, showing that the ions exert a certain pressure on the water as discussed in detail above in Section A.

#### E) Self Diffusion Coefficient for Water

The self diffusion coefficient for the water molecules in the CsCl solution calculated here using the relationship

$$D = \lim_{t \rightarrow \infty} \left\langle \frac{[R(t) - R(0)]^2}{6t} \right\rangle$$

leads to a value of  $7.2 \cdot 10^{-5}$  cm<sup>2</sup>/sec. There exists a large discrepancy between this value and the one obtained by Endom, Hertz, Thül and Zeidler<sup>10</sup> from NMR measurements. They found the  $D$  value for water in a 2 M CsCl solution to be  $2.78 \cdot 10^{-5}$  cm<sup>2</sup>/sec at 25 °C.

The self diffusion coefficient calculated here for the CsCl solution corresponds to a molecular dynamics value for pure water at 97 °C<sup>4</sup>. Contrary to the discrepancy found for the CsCl solution the agreement for pure water at 25 °C between molecu-

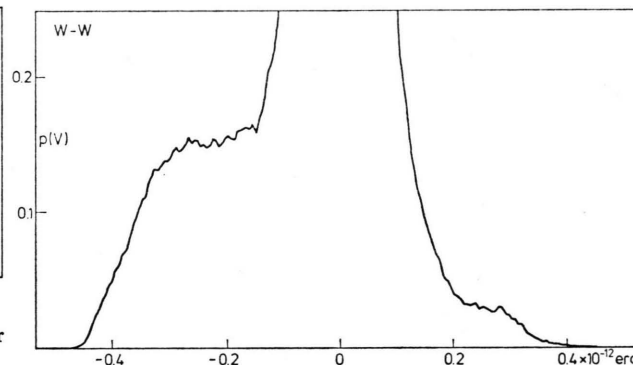


Fig. 12. Pair interaction energy distribution function for water-water.  $p(V)$  is given in arbitrary units.

lar dynamics calculations and experimental results is reasonably good. By interpolation of the data from Stillinger and Rahman<sup>3</sup>  $D \cdot 10^5$  [cm<sup>2</sup>/sec] is determined to be 2.8 while the measured values are 2.6<sup>12</sup>, 2.5<sup>10</sup> and 2.3<sup>11</sup>. For pure water as well as for the CsCl solution the ST2 water model is employed in the calculations. There is no convenient explanation for this discrepancy.

#### V. Concluding Remarks

Adhering to the ST2 water model further improvements in the effective pair potentials seem only to be possible, as far as the ion-ion interaction is concerned, by including 124 instead of 26 nearest neighbour image boxes. On the basis of this improvements a comparison of various alkali halide solutions in respect to the properties calculated here seems to be justified for these concentrations. Furthermore, calculations at lower concentrations appear to be reasonable at this stage. With improved simulation an increase in the number calculated properties should go parallel.

The question if the ST2 water model is appropriate for ionic solutions or if other models such as the central force model by Lemberg and Stillinger<sup>13</sup> are more adequate remains to be seen.

#### Acknowledgements

Stimulating discussions with Prof Dr. A. Klemm and Dr. L. Schäfer are gratefully acknowledged.

<sup>1</sup> K. Heinzinger and P. C. Vogel, Z. Naturforsch. **29 a**, 1164 [1974].

<sup>2</sup> A. Rahman and F. H. Stillinger, J. Chem. Phys. **55**, 3336 [1971].

- <sup>3</sup> F. H. Stillinger and A. Rahman, J. Chem. Phys. **60**, 1545 [1974].
- <sup>4</sup> F. H. Stillinger and A. Rahman, J. Chem. Phys. **61**, 4973 [1974].
- <sup>5</sup> C. L. Kong, J. Chem. Phys. **59**, 2464 [1973].
- <sup>6</sup> W. Hogervorst, Physica **51**, 59, 77 [1971].
- <sup>7</sup> J. O. M. Bockris and P. P. S. Saluja, J. Phys. Chem. **76**, 2298 [1972].
- <sup>8</sup> H. Bertagnolli, J. U. Weidner, and H. W. Zimmermann, Ber. Bunsenges. **78**, 2 [1974].
- <sup>9</sup> A. H. Narten, F. Vaslow, and H. A. Levy, J. Chem. Phys. **58**, 5017 [1973].
- <sup>10</sup> L. Endom, H. G. Hertz, B. Thül, and M. D. Zeidler, Ber. Bunsenges. **71**, 1008 [1967].
- <sup>11</sup> R. Mills, J. Phys. Chem. **77**, 685 [1973].
- <sup>12</sup> I. H. Wang, J. Phys. Chem. **69**, 4412 [1965].
- <sup>13</sup> H. L. Lemberg and F. H. Stillinger, J. Chem. Phys. **62**, 1677 [1975].